PHYSICS TEXTBOOK

Volker Beckmann , Chris Shrader

WILEY-VCH

Active Galactic Nuclei

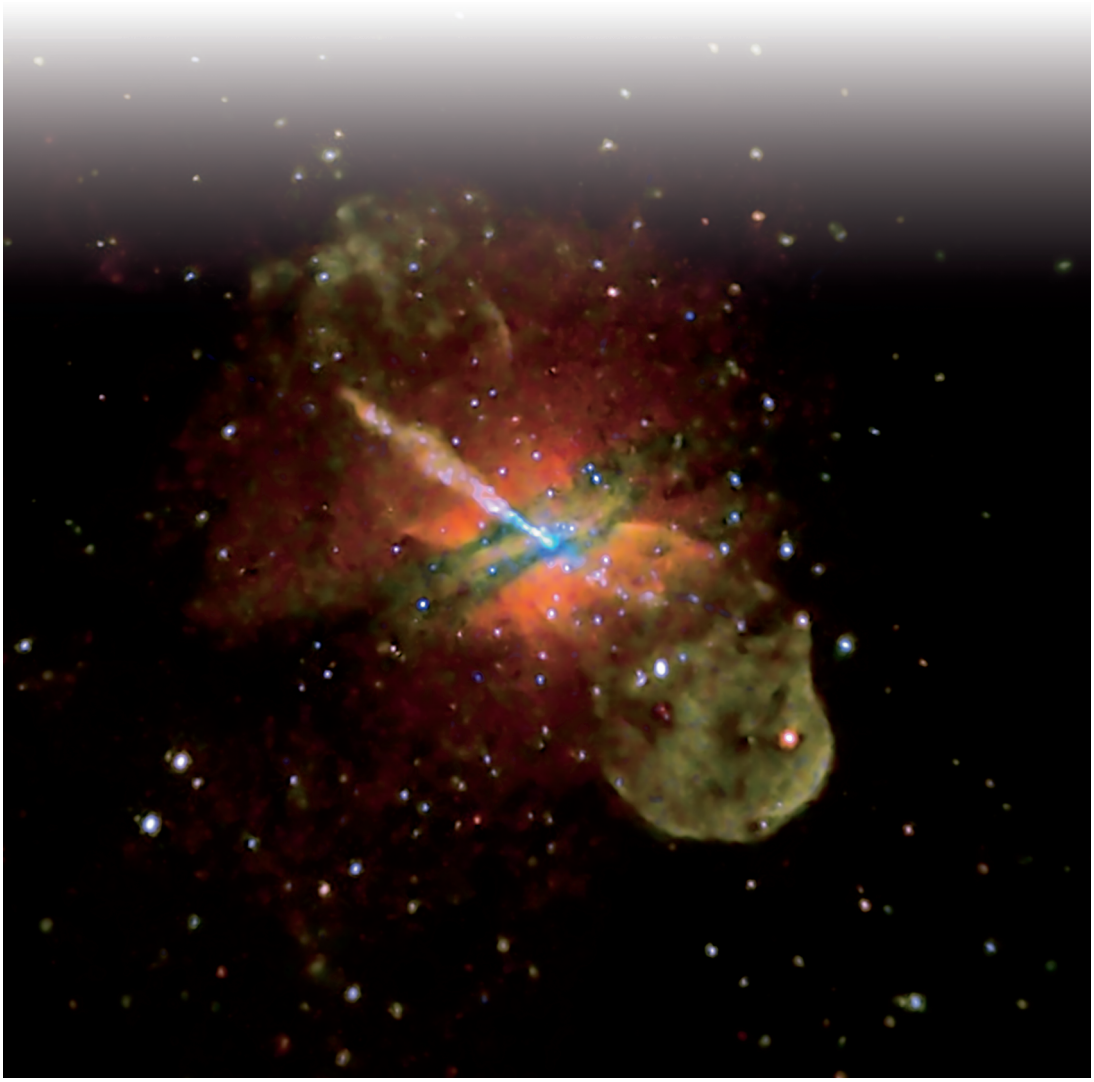

Volker Beckmann and Chris Shrader

Active Galactic Nuclei

Related Titles

von Berlepsch, R. (ed.)

Reviews in Modern Astronomy Vol. 22
Deciphering the Universe through Spectroscopy

2011
ISBN: 978-3-527-41055-2

Röser, S. (ed.)

Formation and Evolution of Cosmic Structures
Reviews in Modern Astronomy Vol. 21

2009
ISBN: 978-3-527-40910-5

Salaris, M., Cassisi, S.

Evolution of Stars and Stellar Populations

2005
ISBN: 978-0-470-09219-4

Phillipps, S.

The Structure and Evolution of Galaxies

2005
ISBN: 978-0-470-85506-5

Rüdiger, G., Hollerbach, R.

The Magnetic Universe
Geophysical and Astrophysical Dynamo Theory

2004
ISBN: 978-3-527-40409-4

Volker Beckmann and Chris Shrader

Active Galactic Nuclei

WILEY-VCH Verlag GmbH & Co. KGaA

The Authors

Dr. Volker Beckmann
APC Laboratory, CNRS/IN2P3
Université Paris Diderot
10 rue Alice Domon et Léonie Duquet
75013 Paris
France

Dr. Chris Shrader
NASA Goddard Space Flight Center and
Universities Space Research Association
Mail Code 661
Greenbelt, MD 20771
USA

Library of Congress Card No.:
applied for

British Library Cataloguing-in-Publication Data:
A catalogue record for this book is available from the British Library.

Bibliographic information published by the Deutsche Nationalbibliothek
The Deutsche Nationalbibliothek lists this publication in the Deutsche Nationalbibliografie; detailed bibliographic data are available on the Internet at http://dnb.d-nb.de.

Cover Design Adam-Design, Weinheim
Typesetting le-tex publishing services GmbH, Leipzig
Printing and Binding Markono Print Media Pte Ltd, Singapore

Printed in Singapore
Printed on acid-free paper

Hardcover ISBN 978-3-527-41091-0
Softcover ISBN 978-3-527-41078-1

Contents

Preface

Active galactic nuclei (AGN) are the most energetic persistent objects in the Universe. Our understanding of them is roughly summarized in Chapter 1. Such a summary will be insufficient, but the goal is to provide an overview of the topic for the newcomer in the field. In Chapter 2 we take a quick tour through the radiative processes which are common in AGN and give the relevant formulas in order to make the arguments in the book understandable. Chapter 3 then discusses our understanding of what mechanisms drive the AGN emission, and what the main elements are, such as the black hole itself, the accretion disk, the broad and narrow line regions, outflowing jets and absorbing material. The different types of AGN are discussed in Chapter 4, including an attempt to explain all different types by the most simple model possible. In Chapter 5 we take a look at AGN in different energy bands, from the radio to the gamma-ray domain, and examine the overall energy output for beamed and nonbeamed sources. In Chapter 6 we will discuss what one can learn from variability studies of AGN. Up to that point we deal with the central engine and its closest surroundings. In Chapter 7 we will then have a look at in what types of galaxies and galaxy clusters supermassive black holes reside and how the AGN is influenced by the host galaxy and how in turn the central engine might affect the star formation in the surrounding medium. In order to understand the role of AGN in the Universe, we briefly discuss the current cosmological model in Chapter 8 and show how AGN can be used as tools for cosmological studies. We then turn in Chapter 9 to the ultimate question of where quasars come from, how they might be formed, and how they evolve. This also includes the aspects of AGN density evolution in time and how this might depend on the type of AGN or the energy range we study. Chapter 10 summarizes the open issues remaining in AGN research, that is, the big questions which still lack a satisfying answer. We hope that the reader will find that stimulating – and that she or he through their own research will contribute to further progress in this thriving field of astrophysics.

The literature about AGN is full of acronyms and abbreviations. We list the most important ones and those which are used in this book starting after the Preface. Finally, the physical and astronomical constants applied in this book are listed. Throughout the book we use cgs units rather than SI, as it is still common practice in astrophysics.

As for any such undertaking as writing a text book covering a broad scientific topic, we heavily relied on the experience and publications of a large number of

scientists. Many of those publications are listed in the bibliography. Some of the textbooks we had at hand when compiling this book, were Osterbrock (1989), Peterson (1997), Kembhavi and Narlikar (1999), Krolik (1999), De Young (2002), and of course Rybicki and Lightman (1986). Throughout the book we point the reader to review articles on certain topics, and give some bibliographic references for further reading. Here we have put an emphasis on recent publications over more established ones. The idea is that the reader will usually find references to earlier work in the most recent publications in a field. We would like to apologize to all the colleagues whose work we have not mentioned or have not given the proper weight in this book.

This book would not have been possible to write without the help, advice of and discussions with many colleagues. Here we would like to thank in particular Chiara Caprini (CEA/Saclay) and Olaf Wucknitz (AIfA Bonn) for their advice on the cosmology chapter, Markos Georganopoulos (UMBC) on jets and radiative processes, Knud Jahnke (MPIA Heidelberg) for many comments on the environment of AGN, Demos Kazanas (NASA/GSFC) for interesting discussions and advice, Ralf Keil for digging out the NLS1 spectrum, Dirk Lorenzen, who knows how to get a book ready for publication, Piotr Lubiński (CAMK Torun) for reading the entire manuscript, Fabio Mattana (APC Paris) for the discussion about synchrotron self-absorption, Marie-Luise Menzel for the artwork on the unified model, Pierre-Olivier Petrucci (LAOG Grenoble) who provided advice on the typology of AGN, Michael Punch (APC Paris) for improving the VHE discussion, Tapio Pursimo (IAC Canary Islands), discussing the AGN phenomenology and appearance, Fabrizio Tavecchio (OAB Merate) for valuable advice on blazars and jets, Marc Türler (ISDC Geneva) who provided input on several topics, Jane Turner (UMBC) for sharing her abundant expertise on the X-ray properties of AGN, Lisa Winter (University of Colorado) for her advice on ultraluminous X-ray sources, and Christian Wolf (Oxford University) for explaining the multiband surveys. Volker thanks his mother for pointing out that NGC 4889 hosts the most massive black hole known to mankind. We also would like to mention the support of our institutions and in particular Pierre Binétruy (APC Paris), Neil Gehrels (NASA/GSFC) and Mike Corcoran (USRA) for their support and encouragement in enabling us to write this book. A very special thank you goes to Simona Soldi (CEA/Saclay), for encouraging the project from the beginning, discussing the context on a daily basis, and correcting the whole manuscript several times.

Of the team at Wiley we would like to thank Oliver Dreissigacker, for contacting us in the first place and thus initiating the AGN book project, Ulrike Fuchs, the commissioning editor, Anja Tschörtner, for helping in the early phase of the project, and Nina Stadthaus, who was a very efficient and friendly editor helping with the technical realization of the project. Finally, we would like to thank Petra Möws and the team at le-tex for their support in the proof-reading process.

Paris and Greenbelt, May 2012 *Volker Beckmann, Chris R. Shrader*

Abbreviations and Acronyms

Here we give the list of the most common acronyms and abbreviations used in this book and in AGN science in general. We caution that the use of abbreviations is not consistent throughout the literature.

ACF	Autocorrelation function
ADAF	Advection-dominated accretion flow
AGN	Active galactic nucleus
ALMA	Atacama Large Millimeter/submillimeter Array
ASCA	Advanced Satellite for Cosmology and Astrophysics
ATHENA	Advanced Telescope for High ENergy Astrophysics
BAL	Broad absorption line quasar
BAO	Baryon acoustic oscillations
BHXRB	Galactic black hole X-ray binary
BLR	Broad-line region
BLRG	Broad-line radio galaxy
BSC	ROSAT All-Sky Survey Bright Source Catalogue
CADIS	Calar Alto Deep Imaging Survey
CCD	Charge-coupled device
CCF	Cross-correlation function
CDF	Chandra Deep Field (X-rays)
CGRO	(Arthur Holley) Compton Gamma-Ray Observatory
CMB	Cosmic microwave background
COMBO-17	Classifying Objects by Medium-Band Observations in 17 Filters
COSMOS	Cosmic Evolution Survey
CTA	Cherenkov Telescope Array
CXB	Cosmic X-ray background
DCF	Discrete cross-correlation function
EBL	Extragalactic background light
EC	External Compton scattering model
EGRET	Energetic Gamma-Ray Experiment Telescope (CGRO)
EMSS	Einstein Observatory Extended Medium Sensitivity Survey
eROSITA	extended ROentgen Survey with an Imaging Telescope Array
EUVE	Extreme Ultraviolet Explorer

EW	Equivalent width
FIRST	Faint Images of the Radio Sky at twenty-centimeters
FR	Fanaroff and Riley
FSRQ	Flat-spectrum radio quasar
FUSE	Far Ultraviolet Spectroscopic Explorer
FWHM	Full-width at half-maximum
GALEX	Galaxy Evolution Explorer
GBH	Galactic black hole
GPS	Gigahertz-peaked spectrum source
HBL	High-frequency cutoff BL Lac object/high frequency peaked BL Lac object
HEAO-2	EINSTEIN satellite
HES	Hamburg/ESO Survey
HPQ	Highly polarized quasar
HQS	Hamburg Quasar Survey
HR	Hardness ratio
HRI	ROSAT High-Resolution Imager
HST	Hubble Space Telescope
HzRG	High-redshift radio galaxy
IACT	Imaging Atmospheric Cherenkov Telescope
IC	Inverse Compton scattering
ICM	Intracluster medium
IBL	Intermediate BL Lac object
IDV	Intraday variability
IGM	Intergalactic medium
IMF	Initial mass function
INTEGRAL	International Gamma-Ray Astrophysics Laboratory
IPC	EINSTEIN Imaging Proportional Counter
IRAS	Infrared Astronomical Satellite
ISO	Infrared Space Observatory
IUE	International Ultraviolet Explorer
LAT	Large Area Telescope (Fermi)
LBL	Low-frequency cutoff BL Lac object/low-frequency peaked BL Lac object
LDDE	Luminosity-dependent density evolution
LECS	Low Energy Concentrator Spectrometer (BeppoSAX)
LF	Luminosity function
LINER	Low-ionization nuclear emission-line region
LISA	Laser Interferometer Space Antenna
LMC	Large Magellanic Cloud
LOFAR	Low Frequency Array (radio)
LSST	Large Synoptic Survey Telescope (optical)
MACHO	Massive compact halo object
mas	Milliarcseconds
MECS	Medium Energy Concentrator Spectrometer

MHD	Magnetohydrodynamics
NED	NASA/IPAC Extragalactic Database
NELG	Narrow-emission-line galaxy
NLR	Narrow-line region
NLRG	Narrow-line radio galaxy
NLS1	Narrow-line Seyfert 1 galaxy
NRAO	National Radio Astronomy Observatory (USA-VA)
NVSS	NRAO VLA Sky Survey
OSSE	Oriented Scintillation Spectrometer Experiment (CGRO)
OVV	Optical violent variable blazar
PAH	Polycyclic aromatic hydrocarbon
PDS	Power Density Spectrum or Phoswich Detector System (BeppoSAX)
PLE	Pure-luminosity evolution
PSF	Point spread function
PSPC	Position Sensitive Proportional Counter (ROSAT)
QPO	Quasiperiodic oscillation
RASS	ROSAT All-Sky Survey
RBL	Radio-selected BL Lac object
ROSAT	Röntgensatellit
RXTE	Rossi X-ray Timing Explorer
SDSS	Sloan Digitized Sky Survey
SED	Spectral energy distribution
SF	Structure function
SIMBAD	Set of Identifications, Measurements, and Bibliography for Astronomical Data
SIS	Solid-State Imaging Spectrometer (ASCA)
SKA	Square Kilometer Array (radio telescope)
SL	Superluminal
SMBH	Supermassive black hole
SMC	Small Magellanic Cloud
SNR	Supernova remnant
SOFIA	Stratospheric Observatory for Infrared Astronomy
SRG	Spectrum-Roentgen-Gamma
SRSQ	Steep radio spectrum quasar
SSC	Synchrotron self-Compton scattering
UHBL	Ultrahigh-frequency peaked BL Lac object
UHECR	Ultrahigh-energy cosmic rays
ULIRG	Ultraluminous infrared galaxy
ULX	Ultraluminous X-ray source
VHE	Very high energy
VLA	Very Large Array (radio)
VLBA	Very Long Baseline Array (radio)
VLBI	Very Long Baseline Interferometry (radio)
VSOP	VLBI Space Observatory Programme

WFI	Wide Field Imager or Wide Field Instrument
WHIM	Warm-hot intergalactic medium
WIMP	Weakly interacting massive particles
XBL	X-ray-selected BL Lac object
XBONG	X-ray bright optically inactive galaxy
XMM	X-ray Multimirror Mission
2MASS	Two-Micron All-Sky Survey

Astronomical and Physical Constants

We list here some astronomical and physical constants which are used throughout the book.

Physical Constants[a)]

Speed of light	c	$2.997\,924\,58 \times 10^{10}$ cm s^{-1}
Planck constant	h	$6.626\,07 \times 10^{-27}$ g cm^2 s^{-1}
Boltzmann's constant	k	$1.380\,65 \times 10^{-16}$ erg K^{-1}
Stefan–Boltzmann constant	σ	5.6704×10^{-5} erg cm^{-2} s^{-1} K^{-4}
Gravitational constant	G	6.6738×10^{-8} cm^3 g^{-1} s^{-2}
Electron mass	m_e	$9.109\,383 \times 10^{-28}$ g
Proton mass	m_p	$1.672\,621\,8 \times 10^{-24}$ g
Neutron mass	m_n	$1.674\,927\,4 \times 10^{-24}$ g
Atomic mass unit	1 u	$1.660\,538 \times 10^{-24}$ g
Elementary charge	e	$1.602\,176\,6 \times 10^{-19}$ C
Electron volt	1 eV	$1.602\,176\,6 \times 10^{-12}$ erg
Fine-structure constant	α	$7.297\,352\,57 \times 10^{-3}$
Wien's displacement constant	b	0.289 777 cm K

[a)] Values taken from the on-line version of Mohr *et al.* (2008).

Astronomical Constants

Solar mass	1 $M_\odot$	1.989×10^{33} g
Solar luminosity	1 $L_\odot$	3.839×10^{33} erg s^{-1}
Astronomical unit	1 AU	1.4960×10^{13} cm
Siderial year	1 yr	$3.155\,815 \times 10^7$ s
Light year	1 ly	9.4605×10^{17} cm
Parsec	1 pc	3.0857×10^{18} cm
		3.2616 ly
Hubble constant	H_0	70.8 km s^{-1} Mpc^{-1}

Color Plates

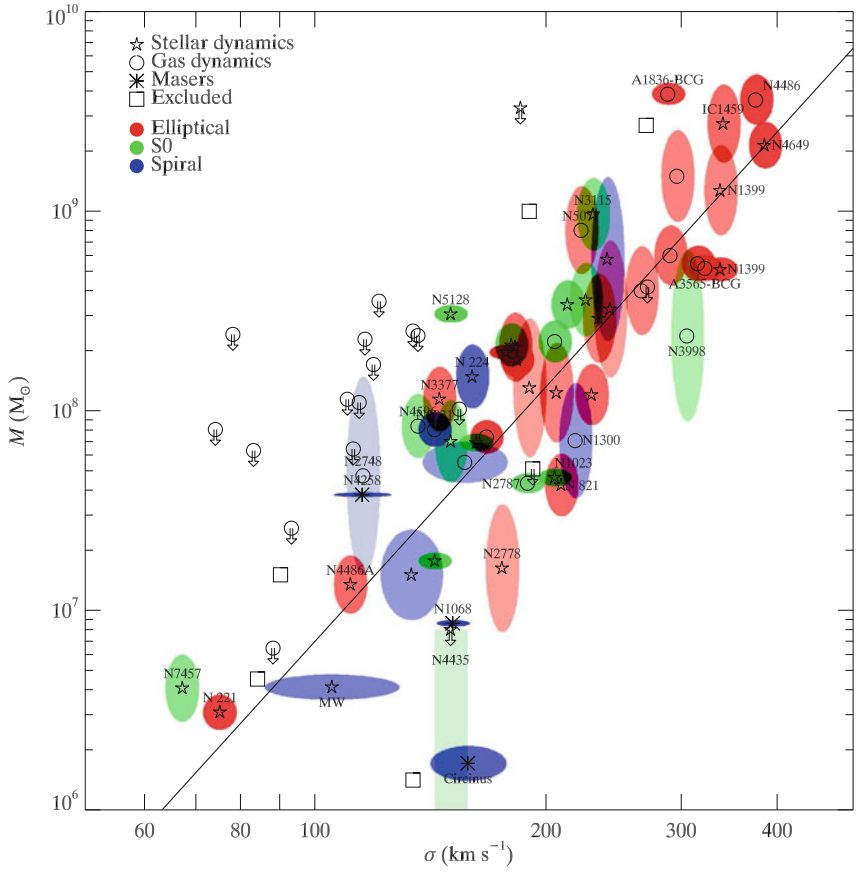

Figure 3.3 This figure illustrates a recent calibration of the $M-\sigma$ relation from Gültekin *et al.* (2009). The colors indicate different galaxy types and the symbols (star, circle and asterisk), indicate the type of black-hole measurement.

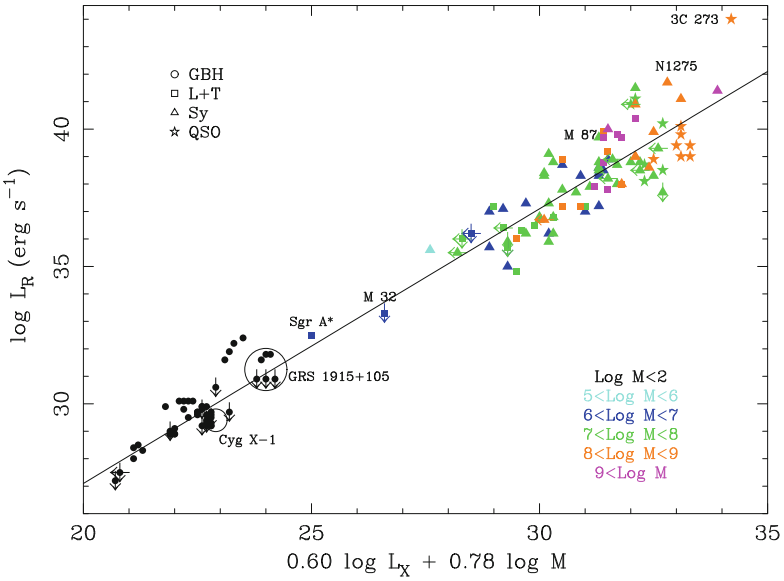

Figure 3.4 The so called Fundamental Plane for accreting black holes with which jet outflows are also associated (Merloni *et al.*, 2003). The observable quantities, L_R and L_X are proxies for the jet and disk power respectively. Objects with mass determinations from other methods were used in constructing this diagram. The tight correlation over many decades of central black hole masses suggests a commonality in the physics underlying the disk-accretion and jet launching mechanism across object sub-classes.

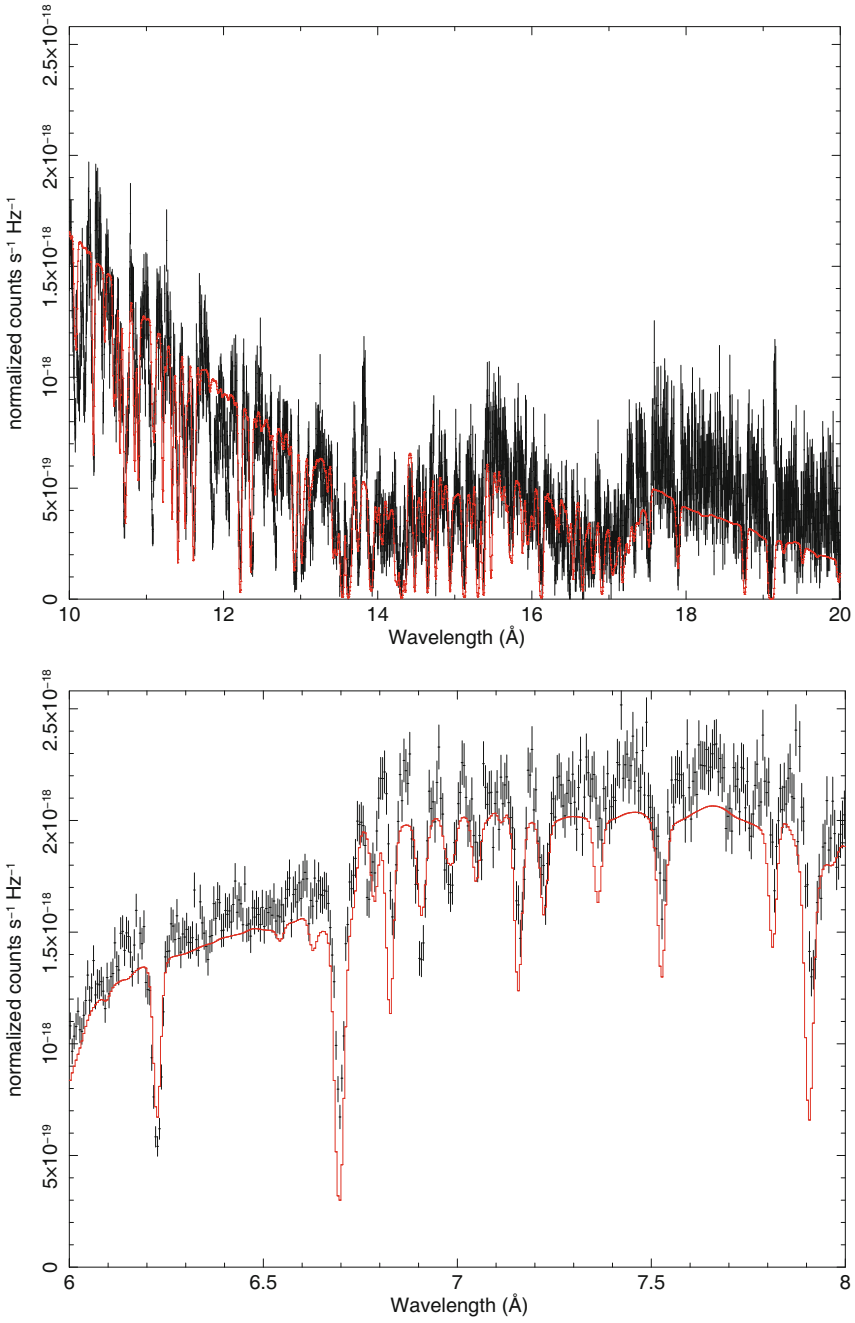

Figure 3.16 Examples of photoionization models of ionized plasma fitted to dispersive X-ray spectra obtained with the Chandra X-ray observatory (Kallman, 2010). The fits led to refinements in iron recombination rates and revealed multiple gas velocity components.

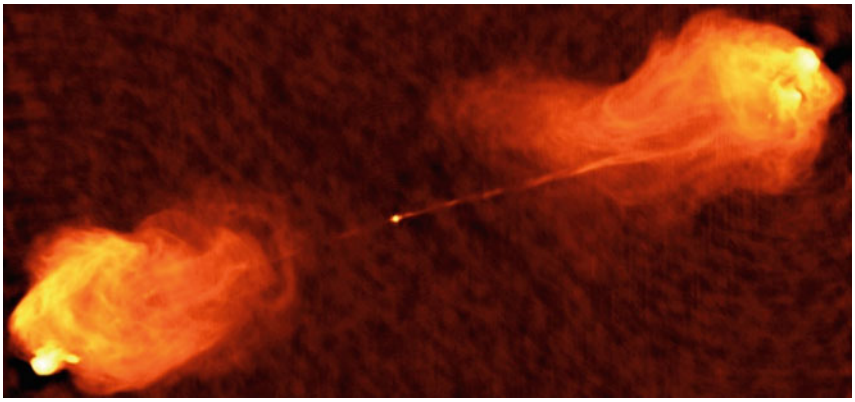

Figure 4.9 The FR-II type radio galaxy Cygnus A is the brightest extragalactic radio source. The picture shows the 5 GHz image taken with the VLA telescope array with 0.4″ resolution (Carilli and Barthel, 1996). The AGN core is located at the bright spot at the center, the radio lobes extend out to about 50 kpc from the core, far beyond the host galaxy which is not visible in the radio domain.

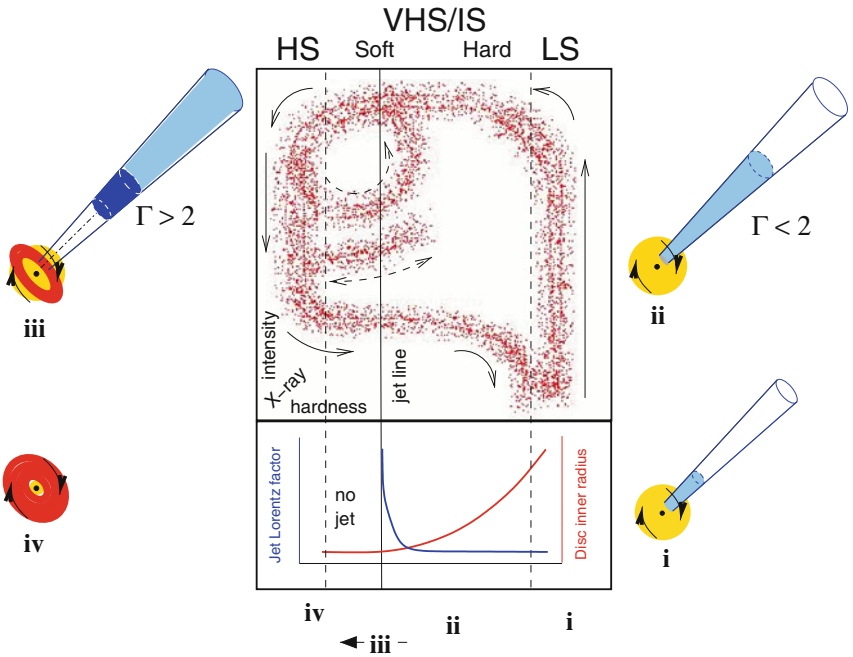

Figure 4.18 Schematic representation of the connection of jet emission, inner disk radius, and spectral state in galactic black hole binaries. The top panel shows the hardness-intensity diagram, in which black holes seems to follow the paths indicated by the arrows. A flat-spectrum radio flux appears and increases with X-ray intensity in the hard state – the rith-hand vertical track of the "q" diagram. The radio emission becomes optically thin and the jet appears as the emission transitions leftwards along the upper horizontal track. The jet disappears after the source moves into the high-soft state. In the bottom panel we see the dependence of jet speed and the inner disk radius on the hardness of the spectrum. X-ray states are indicated with HS (high/soft state), VHS/IS (very high and intermediate state), and LS (low/hard state). The sketches around the outside illustrate the concept of the relative contributions of jet, corona (light grey) and accretion disc (dark grey) at these different stages. Graphic from Fender *et al.* (2004).

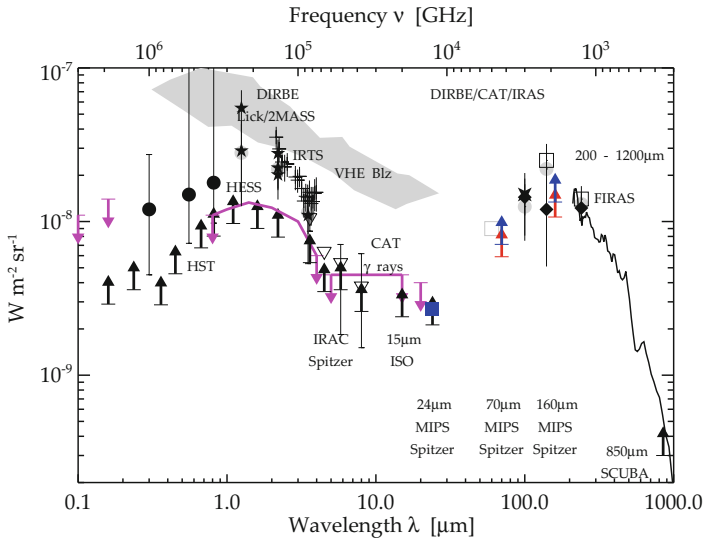

Figure 5.16 The Extragalactic Background Light (EBL) in the optical to infrared range, based on photometric measurements and on indirect techniques (Dole *et al.*, 2006; reproduced with permission © ESO). The HESS TeV data of blazars put strong constraints on the EBL in the range $\lambda = 0.8$—4 μm (indicated by a line).

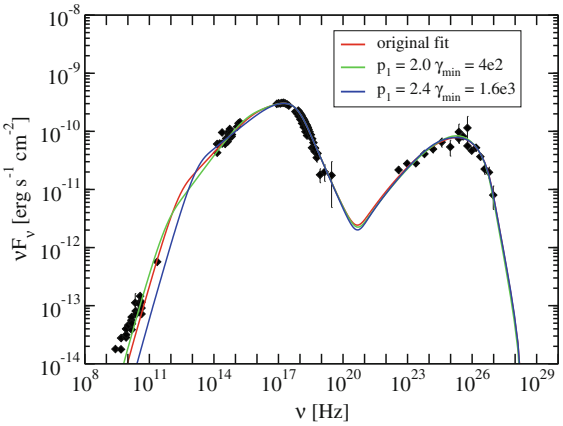

Figure 5.19 SSC model fit of the spectral energy distribution of Mrk 421 based on simultaneous data during a quiescent state of the source. Graphic from Abdo *et al.* (2011b), reproduced by permission of the AAS.

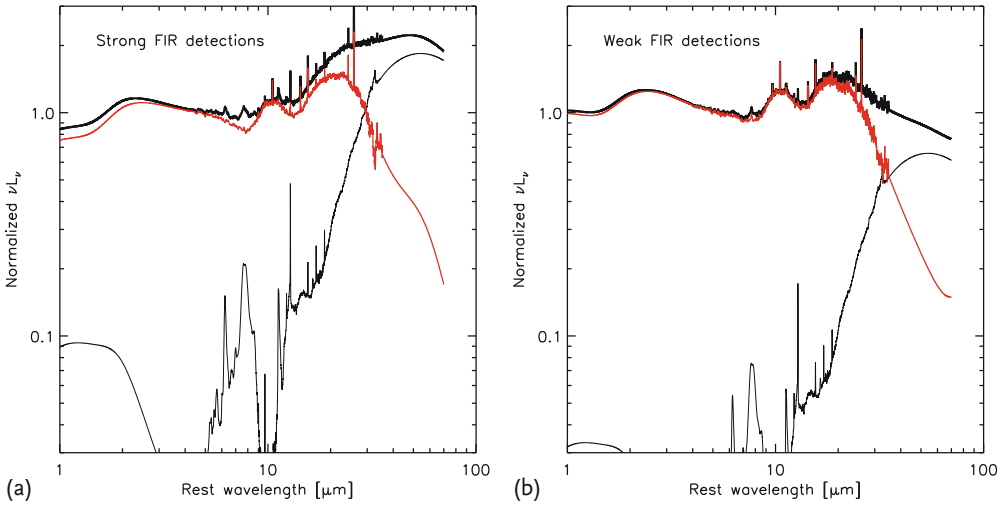

Figure 5.22 Normalized mean SEDs for strong far-infrared (FIR) emitting quasars (a, top curve) and weak FIR quasars (b, top curve). The adjacent red SED curves show "intrinsic" AGN SEDs obtained by the subtraction of the scaled mean starburst (ULIRG) spectrum (shown as the lowest curve in black) from the mean SEDs. From Netzer *et al.* (2007), reproduced by permission of the AAS.

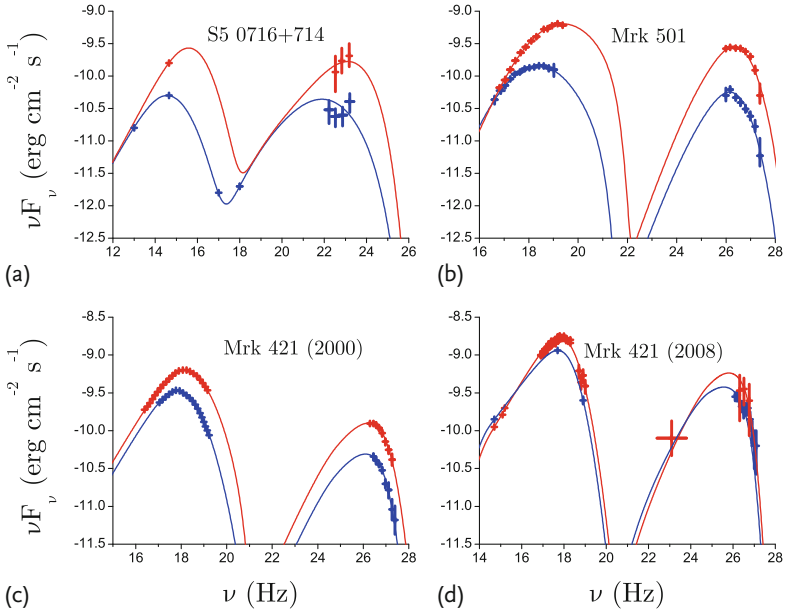

Figure 6.7 Examples for variability of the spectral energy distribution in blazars in low and high emission states. Blazars tend to shift the peak of the synchrotron and inverse Compton branch to higher frequencies, while when comparing different blazars, usually the ones with higher peak frequencies are the less luminous ones as discussed in Section 5.8.1. Graphic from Paggi *et al.* (2009), reproduced with permission © ESO.

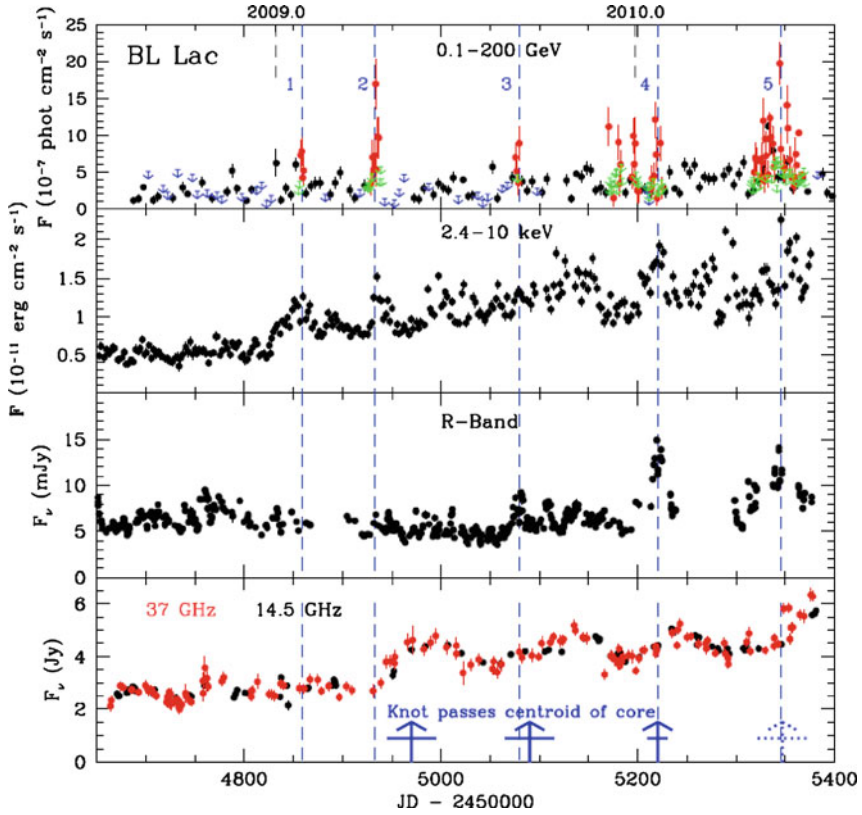

Figure 6.9 Multi-wavelength lightcurve of BL Lac (Marscher *et al.*, 2011). As described in the text, patterns are beginning to emerge between the radio intensity, morphological evolution and flaring at X- and gamma-ray bands. Additional information is potentially forthcoming from comparing polarization measurements of individual jet components to optical polarization of flaring features; specifically, discrete increases in polarization are expected to coincide with gamma-ray flares. The gamma-ray peaks are sharp, and coincide with the rising phase of the radio flux. The radio peaks lag behind the gamma-ray peaks by days to weeks. The VLBA images, not shown here, indicate that the jet knots usually pass through the position corresponding to the radio core concurrently with the gamma-ray flares (vertical arrows).

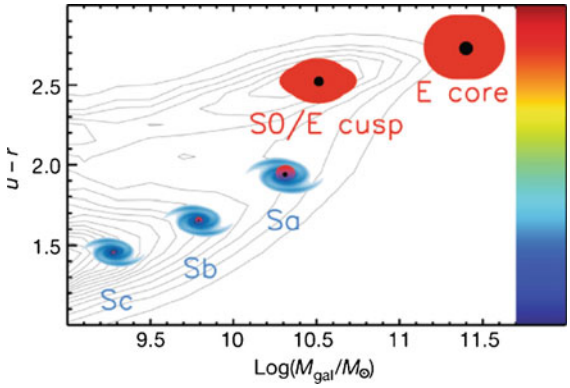

Figure 7.4 Color $u-r$ versus galaxy mass. The larger the $u-r$ value, the redder the galaxy. The central bulge of the spirals are similar to small elliptical galaxies. Ellipticals and spiral bulges have similar stellar mass to black hole mass ratio of the order of 0.1%. Ellipticals are located above a critical mass of $M_{\rm crit} \simeq 10^{12}\, M_{\odot}$. Graphic from Cattaneo *et al.* (2009).

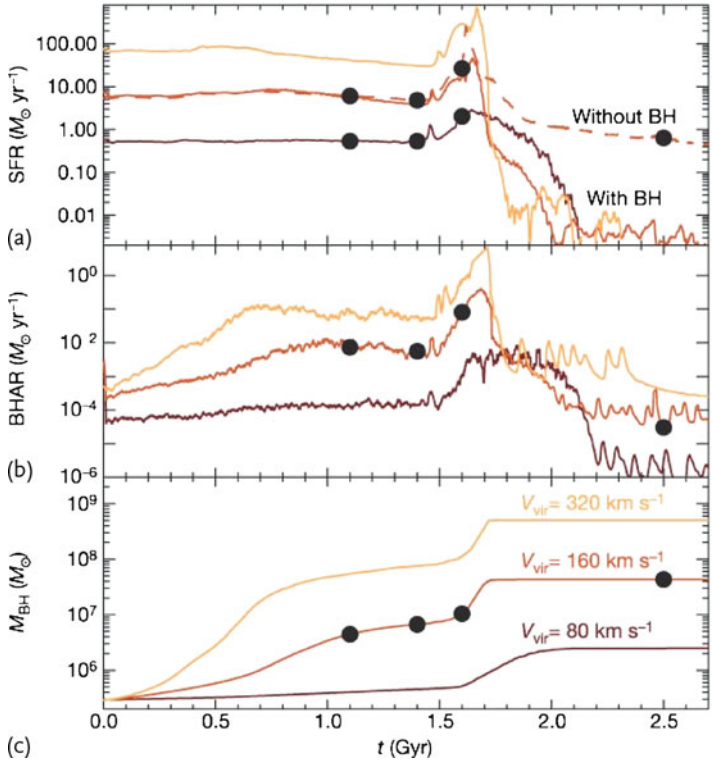

Figure 7.6 Star formation rate (SFR), black hole mass accretion rate (BHAR) and black hole mass for a simulated merging event between two galaxies containing each a super massive black hole about the size of the one in our Galaxy. For comparison, in the upper most panel also the evolution of SFR for a merger without central black holes is shown. Cases of different virial velocity are given. The dots indicate specific times in the merging process. From left to right: first passage of the two galaxies, tidal interaction just before merging, coalescence, and after the merging process has finished. In this graphic from Di Matteo *et al.* (2005) a feedback on the SFR is assumed in the sense that the AGN shuts off the creation of new stars, a scenario disputed for example by Debuhr *et al.* (2010) who argue that the AGN has an impact only on the innermost part of the bulge.

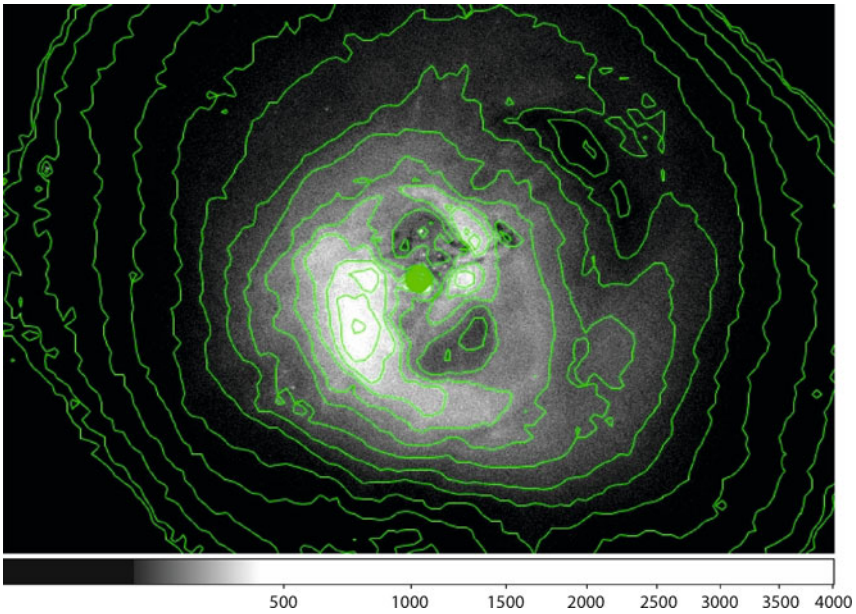

Figure 7.7 The Perseus Cluster as seen by the Chandra X-ray telescope. The center of the cluster is dominated by the emission of the Seyfert and radio galaxy NGC 1275. North and south of the AGN, cavities are visible as well as a larger dark bubble in the northwest. Chandra data obtained from the High Energy Astrophysics Science Archive Research Center (HEASARC), provided by NASA's Goddard Space Flight Center.